Research Paper

Use of a sol-gel hybrid coating composed by a fluoropolymer and silica for the mitigation of mineral fouling in heat exchangers

Valeria Oldani,[a, b, *] Gabriele Sergi,[a] Carlo Pirola,[a, b] Claudia L. Bianchi [a, b]

[a] Dipartimento di Chimica, Università degli Studi di Milano, via C. Golgi 19, 20133 Milano, Italy
[b] Consorzio INSTM, via G. Giusti 9, 50121 Firenze, Italy

ARTICLE INFO

ABSTRACT

The technology of the organic/inorganic hybrid coating was employed in the preparation of a hydrophobic coating (contact angle higher than 140°) for fouling mitigation on stainless steel heat transfer surfaces. A commercial triethoxysilane perfluoropolyethers was combined with a sol-gel silica network with the aim to increase the mechanical and thermal resistance of the films when exposed to aggressive liquid environments as the heat exchanging fluids. The experimentation on a shell and tube heat exchanger pilot plant confirmed the ability of the hybrid coating to prolong the crystallization fouling induction period of 200 h in respect to an uncoated heat exchanger, operating in the same conditions. Moreover, the fouling particles deposited on the coated heat transfer surfaces had only slight adhesion strength toward the coated surfaces and were easily removed by inducing higher wall shear stresses inside the tubes of the plant.

© 2016 Published by Elsevier Ltd.

1. Introduction

Heat exchangers provide the perfect conditions for fouling; the heat exchanging fluids often contain dispersed or dissolved particles, which can adhere on the heat transfer surfaces, and the working temperatures are in general favourable for microorganism proliferation. The main effects of fouling in heat exchangers can be summarized as the increase of the overall heat transfer resistance and the increase of the pressure drop due to the reduction of the cross-sectional flow area, which means losses in the heat transfer efficiency [1,2]. Among all the possible techniques available for fouling control in heat exchangers, the use of metal surfaces, which do not suffer from deposition phenomena, would be certainly one of the best options [3]. To achieve this goal, an anti-fouling coating can be applied on the heat transfer surfaces. Many researches attest in particular the effectiveness of hydrophobic coatings on mitigation of crystallization fouling in heat exchangers [4–7]. Crystallization fouling is one of the most common types of fouling involving heat exchangers and consists in the precipitation and deposition of dissolved salts, after the supersaturation [8].

The preparation of anti-fouling coatings for application on heat transfer surfaces, however, is not trivial [9]. Beside the typical properties of mechanical, chemical and thermal stability, anti-fouling coatings for heat exchangers should not represent a further heat transfer resistance, hence their thickness have to be maintained lower than 5 μm to ensure no insulator effects [3]. Moreover, the effect of the coatings on the average surface roughness should be controlled; the

average roughness of the heat transfer surface can in fact greatly influence the flow regime of the fluid in contact with the heat surface as well as the extent of the fouling phenomenon [10,11].

The organic/inorganic hybrid coating technology can contribute to the obtainment of an anti-fouling coating with the properties just discussed. The careful combination of an organic compound with an inorganic one permits in fact the obtainment of a composite material possessing both the typical properties of the two components [12].

Several reviews [13–15] attest the efficiency of the hybrid coating technology in the mitigation of bio-fouling. Even so, only few researches report the effects of the use of hybrid coatings in the mitigation of other types of fouling phenomena, such as mineral fouling, corrosion fouling or crude oil fouling, especially in heat transfer equipment. Cai et al. [16] studied a composite coating composed by titanium dioxide nanoparticles and fluoroalkylsilane, observing a lower fouling resistance in pool boiling saturated by $CaCO_3$ in presence of the coating. Holberg and Bischoff [17] reported the application of hybrid coatings composed by an urea-siloxane systems. By the optimization of the synthesis, the authors obtained a mechanical robust hybrid coating with proven ability to repel crude-oil derived foulants on heat transfer surfaces.

In this research, we implemented an easy to handle procedure for the preparation of the coating, employing the well-known sol-gel synthetic technique. The procedure includes the co-condensation of tetraethyl orthosilicate, the precursor for silica coating preparation, with a triethoxysilane α,ω-substituted perfluoropolyether. This synthetic approach permits to intersperse homogeneously the inorganic phase (SiO_2) in the organic one, without compromising the typical properties of the polymer [18]. Hence, we obtained a stable hydrophobic coating based on the fluoropolymer [19] with enhanced thermal and mechanical stability conferred by the presence of the metal oxide, which possesses superior mechanical properties in re-

* Corresponding author at: Università degli Studi di Milano, via G. Golgi 19, 20133 Milano, Italy.
Email address: valeria.oldani@unimi.it (V. Oldani)

spect to polymers [20]. The mechanical and chemical stability of the hybrid coating prepared in this work were investigated in liquid media, using chemically aggressive solutions and high temperatures to simulate the exposition to heat exchanging fluids. The anti-fouling properties, instead, were evaluated in a heat exchanger pilot plant, operating with water rich in carbonate salts responsible of crystallization fouling phenomena.

2. Material and methods

2.1. Coatings synthesis and preparation

The hybrid coating (briefly named $S10/SiO_2$) was prepared by combining a sol-gel silica coating and a perfluoropolyether derivative. The silica coating was prepared by classical sol-gel synthesis starting from the alkoxide precursor (TEOS), as reported by Kermadi et al. [21]. The commercial perfluoropolyether (named Fluorolink®S10, provided by Solvay Specialty Polymers) was mixed with TEOS, maintaining a weight ratio of 80/20 respectively, before the initiation of the hydrolysis and condensation reaction. iso-propanol was used as solvent in the sol-gel synthesis, the amount of solvent was maintained in large excess in order to reduce the viscosity of the sol-gel. The amount of S10 in respect to the solvent was 2.7 wt%. Water was added in the molar ratio of 4.0/1.0 in respect to TEOS, and pH was regulated at a value of 2 using nitric acid. The sol-gel synthesis was performed at room temperature, maintaining the solution under stirring for 24 h. The coatings were deposited on stainless steel substrates (plain samples of dimensions 30 × 20 mm or tubes samples with internal diameter of 8 mm and length 100 mm) via dip-coating. Namely, the substrates were kept immersed in the coating solution for 3 h and heat treated for 3 h at 383 K and for 1 h at 473 K in a static oven. Before the coating deposition, the stainless steel substrates were rinsed with water and acetone. Similarly, the tube bundle of the heat exchanger pilot plant was carefully washed with water and acetone and consequently dipped in the coating formulation (using a tank of 8 L volume) for 3 h. The heat treatment was performed as previously described.

2.2. Resistance and fouling tests

The hybrid coating prepared was preliminary studied to assess its resistance when exposed to liquids simulating the heat exchanging fluids. Plain stainless steel substrates where used as samples for the resistance tests. The chemical stability was investigated by immersing the samples in a hydrochloric acid solution (HCl, pH = 2), a disinfectant solution containing chloramines (pH = 7), and a synthetic seawater solution. During the tests, all the solutions were thermostated at a temperature of 323 K. The thermal resistance was assessed by exposing the samples to water heated at 343 K. The mechanical resistance was instead investigated by exposing the samples to a water flow, at a temperature of 323 K, and velocity of 0.17 m/s. A similar test was performed using a solution of $CaSO_4$, 4 g/L concentrated, instead of water. In that case, the $CaSO_4$ solution, pre-heated at a temperature of 313 K, was pumped (flowrate: 0.15 m/s) in a tubular stainless steel sample characterized by the presence of the coating on its internal surface. In such a way it was possible to assess the wear resistance of the coatings in presence of a solution rich in suspended particles. The apparatus used for the latter tests are described elsewhere [22]. All the resistance tests lasted for 30 days, apart from the test performed in presence of the $CaSO_4$ solution, which lasted for 43 days. The testing liquids where replaced periodically every 2/3 days, in order to maintain unaltered the environmental conditions to which the samples where exposed. The same resistance test was repeated at least two times, using different coated samples.

The deterioration of the coatings was monitored by measuring the water contact angle value of the coated substrates (Kruss Easydrop instrument). For each sample, at least 5 droplets where deposited on different position of the surface, and the CA value was calculated as the average of these measurements. A decrease in the CA value was representive of a deterioration of the coating.

The anti-fouling ability of the hybrid coating $S10/SiO_2$ was investigated on real heat transfer surfaces, by the aim of a heat exchanger pilot plant. The schematic of the plant is reported in Fig. 1.

The pilot plant is composed by two shell and tube heat exchangers (STHX), TEMA type NEW, working in parallel and designed identically. During the experimentation, only the tube bundle of STHX A was coated. Each heat exchanger is equipped with control devices (Table 1), which permitted the recording of the temperatures of the inlet and outlet fluids, in both shell side and tube side. The flowrates of the inlet fluids in shells and tubes were regulated using float flowmeters (see Table 1).

Table 2 reports in brief some specifications concerning the design of the two shell and tube heat exchangers.

Tap water, provided from the water system of the city of Milan, was used as operating fluid. The amount of calcium and magnesium measured in a sample of water corresponded to 76 mg/L and 18 mg/L respectively, therefore we supposed that the main fouling mechanism involved during the experiment was crystallization fouling. In fact, in a previous work, involving a similar apparatus working in analogous conditions, we clearly observed the formation of scale deposits on the
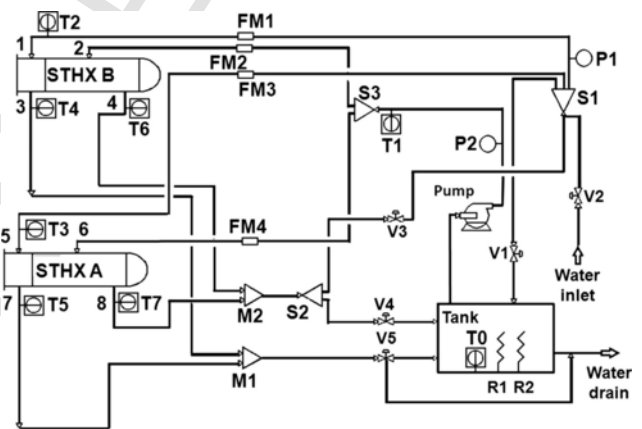

Fig. 1. Flowsheet of the heat exchanger pilot plant. STHX A, coated heat exchanger; STHX B, uncoated heat exchanger; FM, flowmeters; M, mixer; P, pressurimeters; R, heating elements; S, splitter; T, thermocouples; V, valves.

Table 1
Description of the operating units and of the analytical devices included in the heat exchanger pilot plant. The symbols adopted correspond to the ones reported in Fig. 1.

Symbol and name	Specifications
FM1/FM2 float flowmeter	Parker, measure range: 12–120 L/h, standard accuracy: ±5% of full scale flow
FM3/FM4 float flowmeter	Key Instruments, measure range: 120–1200 L/h, standard accuracy: ±5% of full scale flow
P1-P4 manometer	INOX, measure range: 0–5 bar
R1/R2 heating elements	230 V, 3 kW, alimented in series
T0 thermocouple	Immersion thermocouple, rigid, for temperature measurement in the hot water tank. Sensibility: 10–50 µV/°C
T1-T4 thermocouples	Contact thermocouple, flexible, sensibility: 10–50 µV/°C
V1-V6 valves	INOX ball valve, certified ISO 9001 and ISO 14001

Table 2
Description of the shell and tube heat exchangers lay-out.

Shell side		Tube side		Further specifications	
Internal diameter	90 mm	Number of tubes	22	Baffles cross	Single segmental
Outside diameter	102 mm	Number of tubes passes per shell	6	Baffle spacing	27 mm
Length	700 mm	Tubes internal diameter	8 mm	Baffle diameter	87 mm
Number of passes per shell	1	Tubes length	700 mm	Flow regime	Counter flow
Material	Aluminium	Tubes layout	30°		
		Material	AISI 316		

heat transfer surfaces [23]. The hot water, collected in the storage tank, was heated at a temperature of 313–323 K by two heating elements and consequently pumped inside the tubes at a flowrate of 720 L/h. The cold fluid, directly coming from the water supply network, flowed inside the shell at a temperature varying from 290 K to 292 K and flowrate 108–120 L/h.

We estimated the Re number in the shell side following the Kern method [24]; it ranged, during the operation, from 1880 to 2090. The Re number in the tube side was 2346; hence, the flow regime involved in the experimentation was mainly laminar. The operating conditions were kept very similar between the two heat exchangers during the experimental work, thus, it was possible to compare the heat transfer efficiency of the coated heat exchanger with the one of the uncoated heat exchanger. In the result section, the variation with time of the overall heat transfer coefficient (U_{lm}) of STHX A is compared with the one of STHX B. The coefficient U_{lm} was calculated according to Eq. (1) [25]:

$$U_{lm} = \frac{Q}{A_{lm} \Delta T_{lm}}$$

(1)

In Eq. (1), Q is the quantity of heat transferred from the hot fluid to the cold one, A_{lm} is the logarithmic mean of the heat transfer surface and ΔT_{lm} is the logarithmic mean of the temperature differences in the shell side and hot side.

Considering the formation of fouling layer prevalently on the internal side of the tubes, we also calculated the fouling resistance R_f, according to Eq. (2) [26]:

$$R_f = \frac{1}{U_t} - \frac{1}{U_0}$$

(2)

where U_t is the overall heat transfer coefficient at the generic time t, while U_0 is the overall heat transfer coefficient at the start of the operation, i.e., when the heat transfer surfaces are supposed to be clean.

3. Results and discussion

3.1. Chemical and mechanical resistance of the hybrid coatings

Fig. 2 sums up the results of resistance tests. Here, the best results of each resistance tests are presented. The average CA value of a fresh coating deposited on the stainless steel substrate was 144° ± 3. On the other hand, typically, a clean and uncoated stainless steel surface has a CA varying from 60° to 80°. Therefore, the decrease in CA
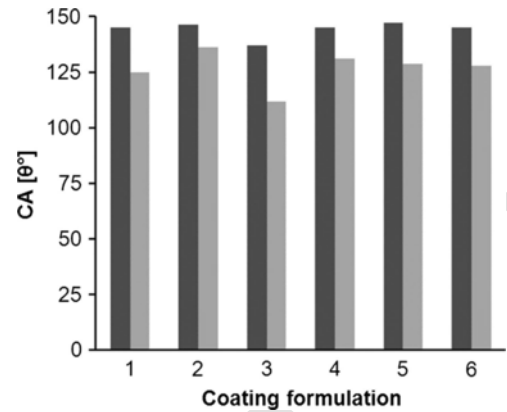

Fig. 2. Results of the resistance tests performed on the hybrid coating S10/SiO$_2$: comparison between the CA measured before the test (■) and at the end of the test, lasted for 30 days (■). Exposition to: 1 = HCl solution, 2 = disinfectant solution, 3 = synthetic seawater solution, 4 = water at 343 K, 5 = water flux at 0.17 m/s, 6 = CaSO$_4$ solution fluxed in a coated tube at 0.15 m/s.

that we observed during the resistance tests was indicative of a progressive deterioration of the coating. The most detrimental solution for the hybrid coatings was represented by the synthetic seawater solution. After 30 days of immersion we observed a consistent decrease of CA (18% in respect to the starting value), corresponding to a final CA value of 112°. On the other hand, the exposition to the other typology of aggressive liquids did not alter consistently the wettability of the coated samples, and the final contact angles measured were always higher than 125°. Interestingly, the hybrid coating appeared highly stable against thermal stresses. The prolonged exposition to water at high temperature brought to a decrease in CA of only the 9%. The hybrid coating demonstrated good mechanical resistance even against shear stresses; the exposition to the water flux and to the CaSO$_4$ solution, fluxed inside the coated tube sample, determined a decrease in CA of the 12% (final contact angle ~125°).

3.2. Fouling mitigation

The heat treatment necessary for the hardening of the hybrid coating was performed at high temperatures (383 K and 473 K). We estimated a linear expansion of the stainless steel tubes due to the thermal gradient induced in the heating treatment of 0.1 mm, which is a negligible value. From surface profilometry analyses (UBM Microfocus Measurement System), we estimated that the average thickness of the coatings that we prepared was 7 µm. Moreover, we observed an increase of the average roughness (Ra) of the stainless steel substrate after the deposition of the coating from 0.749 µm to 0.953 µm (roughness was measured by profilometer analysis, UBM Microfocus Measurement System, on an area of 0.3 × 0.5 mm and resolution of 500 points/mm).

The fouling mitigation effect of the hybrid coating can be observed comparing the overall heat transfer coefficient and the fouling resistance values calculated for the uncoated heat exchanger (STHX B), with the ones of the coated heat exchanger (STHX A), as presented in Figs. 3 and 4. The scattering of the experimental values observable in these figures is mainly due to the continuous variation of the temperatures and of the flowrates in the range reported in Section 2.2. The variation of these parameters involved simultaneously the two heat exchangers, which worked in parallel and in the same conditions for the whole duration of the experiment (580 h). Each U_{lm} or R_f value presented in Figs. 3 and 4 correspond to the average daily value, calculated from the data collected 8 times/day.
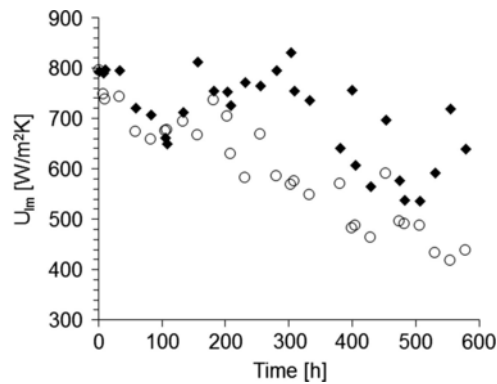
Fig. 3. Comparison between the values of the overall heat transfer coefficient U of the coated heat exchanger STHX A (◆) and the uncoated heat exchanger STHX B (○).
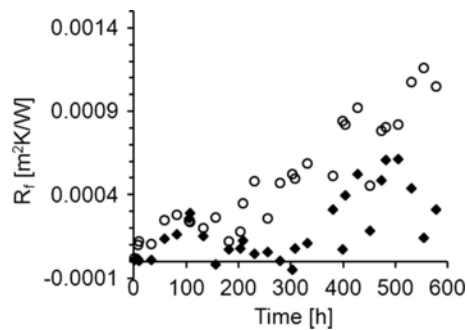

Fig. 4. Comparison between the fouling resistance (R_f) values of the coated heat exchanger STHX A (◆) and the uncoated heat exchanger STHX B (○).

Fig. 3 emphasizes the variation with time of U_{lm} in STHX A and STHX B. The initial U_{lm} values of STHX A and B were very similar, 793 and 795 W/m² K respectively, hence we can suppose that in the apparatus described, the influence of the hybrid coating on the heat transfer ability of the stainless steel surface was negligible. Until 200 h of operation the U_{lm} value of STHX A and B remained almost similar. The average U_{lm} value in the period 0–200 h for STHX A was 756 W/m² K and for STHX B 715 W/m² K. After 200 h of operation, the overall heat transfer coefficient of STHX B started to decrease, while the U_{lm} values of STHX A remained almost unvaried. The average value of U_{lm} in the period comprised between 200 and 400 h was in fact 769 W/m² K for STHX A and 598 W/m² K for STHX B. Hence, a consistent decrease of the heat transfer capacity of the uncoated heat exchanger was observed after 200 h of operation. Hypothetically, the progressive reduction in the overall heat transfer coefficient observed in the uncoated heat exchanger was due to the formation of scale deposits on the heat transfer surfaces. On the other hand, the hydrophobic coating prevented the scale deposition on the heat transfer surfaces of STHX A until, at least, 400 h of operation. In fact, the U_{lm} value of the coated heat exchanger decreased with a similar extent after ~400 h of operation (During the working period of 400–550 h U_{lm} was in fact 598 W/m² K). At the same time, we observed that the overall heat transfer coefficient of the uncoated heat exchanger continued to decrease, the average value of U_{lm} calculated from 400 to 550 h of operation was in fact 493 W/m² K.

After 550 h of experiment, the pilot plant was shut down to permit the removal of the scale deposits formed on the heating units placed in the tank. The operation lasted for several hours and during that interval the two heat exchangers were completely emptied. After the maintenance procedure, the experimentation started again and proceeded for 80 more hours. During that period we observed a progres-

sive restore of the initial U_{lm} value in the coated heat exchanger (average U_{lm} value in the period of operation 500–580 h was 687 W/m² K). A similar result was not observed in the uncoated heat exchanger, the average U_{lm} value in the same period was in fact 425 W/m² K. The restoring of the initial heat transfer conditions observed in STHX A can be related to the hydrophobic/anti-fouling effect of the hybrid coating, which made difficult the adhesion of the foulant particles on the internal surfaces of the tubes. Hence, inducing wall shear stresses, the removal of the scale deposits was favored by the presence of the hybrid coating.

The assumptions made from the analyses of the U_{lm} values in the two heat exchangers can be confirmed from the observation of the fouling resistance (R_f) trends (Fig. 4).

The fouling resistance values remained very similar between the two heat transfer plants until 200 h of operation ($9 \cdot 10^{-5}$ *vs* $1 \cdot 10^{-4}$ m² K/W for STHX A and B respectively). An increase of the R_f value was observed for STHX B in the operating period comprised between 200 and 400 h, in fact the average value rose at $4 \cdot 10^{-4}$ m² K/W. On the contrary, the fouling resistance remained almost unvaried for STHX A ($7 \cdot 10^{-5}$ m² K/W). Therefore, we can suppose a shift from the fouling induction period to the fouling period in the uncoated heat exchanger after 200 h of operation. A consistent rise of the fouling resistance in the coated heat exchanger was instead observed after 400 h of operation; the average R_f value calculated between 400 and 500 h of working was in fact $5 \cdot 10^{-4}$ m² K/W. Hence, the hydrophobic coating was able to prolong the fouling induction period of about 200 h in the conditions here adopted. Moreover, after the maintenance procedure, involving the shutdown of the pilot plant, we observed a decrease of the fouling resistance in the coated heat exchanger (the average value in the period of operation of 500–580 h was $2 \cdot 10^{-4}$ m² K/W). This result can be explained by the removal of the fouling particles thanks to a wall shear stress effect, induced in the step of refilling of the heat exchanger. The same phenomenon was not observed on the uncoated heat exchanger, where the foulant particles had the possibility to adhere much strongly to the stainless steel surface. In fact, the average R_f value in the last working period was $1 \cdot 10^{-3}$ m² K/W.

4. Conclusions

We evaluated the applicability of a hybrid coating composed by a perfluoropolyether and a sol-gel silica network in fouling mitigation in heat exchangers. The synthetic procedure implemented involves an established technology for the industrial production of coatings, as the sol-gel procedure, and uses as raw material commercially available products, with the aim to scale-up such a technology. The main conclusions are the follow ones:

(1) The hybrid coating demonstrated the ability to reduce fouling due to scale on heat transfer surfaces. The fouling induction period was prolonged of about 200 h on coated heat transfer surfaces as evinced by the experimentation performed on a heat exchanger plant in pilot scale. Moreover, the coating improved the removal of the fouling deposits under wall shear stresses.

(2) The hybrid coating (having an average thickness of 7 μm) only scarcely affected the heat transfer ability of the stainless steel surfaces. However, we observed an increase of the average roughness of the stainless steel substrate of about 2.0 μm after the deposition of the coating.

A selective study on the roughness variation, due to the coating deposition, on substrates having different Ra starting values, in respect to the one selected for this research, has not been performed yet. However, it is important to consider this effect in design step of the heat exchanger.

(3) Such a results were obtained maintaining relative mild conditions in the pilot plant. Hard water was used as heat exchanging fluid, laminar flow conditions were maintained both in shell and tubes and small temperature differences ($\Delta T = 30$ K) occurred between the hot and cold fluid. For this reason, to obtain more precise results on the effectiveness of the SiO_2/S10 hybrid coating in fouling mitigation, further investigations should be made varying the temperature ranges and the flow regimes, by adjusting the design of the heat exchanger pilot plant.

Acknowledgments

References

[1] M. Markowski, M. Trafczynski, K. Urbaniec, Identification of the influence of fouling on the heat recovery in a network of shell and tube heat exchangers, Appl. Energy 102 (2013) 755–764.

[2] H. Müller-Steinhagen, M.R. Malayeri, P. Watkinson, Heat exchanger fouling: mitigation and cleaning strategies, Heat Transfer Eng. 32 (2011) 189–196.

[3] H. Müller-Steinhagen, Q. Zhao, Investigation of low fouling surface alloys made by ion implantation technology, Chem. Eng. Sci. 52 (1997) 3321–3332.

[4] A. Marmur, Super-hydrophobicity fundamentals: implications to biofouling prevention, Biofouling 22 (2006) 107–115.

[5] Q. Zhao, Y. Liu, C. Wang, S. Wang, H. Müller-Steinhagen, Effect of surface free energy on the adhesion of bio-fouling and crystalline fouling, Chem. Eng. Sci. 60 (2005) 4858–4865.

[6] Y.H. Cheng, H.Y. Chen, Z.C. Zhu, T.C. Jen, Y.X. Peng, Experimental study on the anti-fouling effects of NiCuP-PTFE deposit surface of heat exchangers, Appl. Therm. Eng. 68 (2014) 20–25.

[7] M. Förster, M. Bohnet, Modification of molecular interactions at the interface crystal/heat transfer surface to minimize heat exchanger fouling, Int. J. Therm. Sci. 39 (2000) 697–708.

[8] S.N. Kazi, K.H. Teng, M.S. Zakaria, E. Sadeghinezhad, M.A. Bakar, Study of mineral fouling mitigation on heat exchanger surface, Desalination 367 (2015) 248–254.

[9] D.J. Kukulka, P. Leising, Evaluation of heat exchanger surface coatings, Appl. Therm. Eng. 30 (2010) 2333–2338.

[10] F. Albert, W. Augustin, S. Scholl, Roughness and constriction effects on heat transfer in crystallization fouling, Chem. Eng. Sci. 66 (2011) 499–509.

[11] A. Herz, M.R. Malayeri, H. Müller-Steinhagen, Fouling of roughened stainless steel surfaces during convective heat transfer to aqueous solutions, Energy Convers. Manage. 49 (2008) 3381–3386.

[12] H. Fischer, Polymer nanocomposites: from fundamental research to specific applications, Mater. Sci. Eng., C 23 (2003) 763–772.

[13] M. Lejars, A. Margaillan, C. Bressy, Fouling release coatings: a nontoxic alternative to biocidal antifouling coatings, Chem. Rev. 112 (2012) 4347–4390.

[14] Y. Tang, J.A. Finlay, G.L. Kowalke, A.E. Meyer, F.V. Bright, M.E. Callow, J.A. Callow, D.E. Wendt, M.R. Detty, Hybrid xerogel films as novel coatings for antifouling and fouling release, Biofouling 21 (2005) 59–71.

[15] J.A. Callow, M.E. Callow, Trends in the development of environmentally friendly fouling-resistant marine coatings, Nat. Commun. 244 (2011) 1–10.

[16] Y. Cai, M. Liu, L. Hui, $CaCO_3$ fouling on microscale–nanoscale hydrophobic titania–fluoroalkylsilane films in pool boiling, AIChE J. 59 (2013) 2662–2678.

[17] S. Holberg, C. Bischoff, Application of a repellent urea–siloxane hybrid coating in the oil industry, Prog. Org. Coat. 77 (2014) 1591–1595.

[18] S. Pandey, S.B. Mishra, Sol–gel derived organic–inorganic hybrid materials: synthesis, characterizations and applications, J. Sol-Gel Sci. Techn. 59 (2011) 73–94.

[19] B. Ameduri, B. Boutevin, J.J.E. Moreau, M. Moutaabbid, M. Wong Chi Man, Hybrid organic±inorganic gels containing perfluoro-alkyl moieties, J. Fluorine Chem. 104 (2000) 185–194.

[20] J.D. Mackenzie, E.P. Bescher, Physical properties of sol-gel coatings, J. Sol-Gel Sci. Techn. 19 (2000) 23–29.

[21] S. Kermadi, N. Agoudjil, S. Sali, M. Boumaour, S. Bourgeois, M.C. Marco de Lucas, Sol-gel synthesis of $xTiO_2(100-x)SiO_2$ nanocomposite thin films: structure, optical and antireflection properties, Thin Solid Films 564 (2014) 170–178.

[22] V. Oldani, R. del Negro, C.L. Bianchi, R. Suriano, S. Turri, C. Pirola, B. Sacchi, Surface properties and anti-fouling assessment of coatings obtained from perfluoropolyethers and ceramic oxides nanopowders deposited on stainless steel, J. Fluorine Chem. 180 (2015) 7–14.

[23] V. Oldani, C.L. Bianchi, S. Biella, C. Pirola, G. Cattaneo, Perfluoropolyethers coatings design for fouling reduction on heat transfer stainless steel surfaces, Heat Transfer Eng. 37 (2016) 210–219.

[24] D.Q. Kern, Process Heat Transfer, International Student Edition, McGrow Hill International Book Company, Tokio, 1983.

[25] A. Dimian, C. Bildea, A. Kiss, Integrated Design and Simulation of Chemical Processes, second ed., Elsevier, Amsterdam, 2014.

[26] M.R. Malayeri, A. Al-Janabi, H. Müller-Steinhagen, Application of nano-modified surfaces for fouling mitigation, Int. J. Energy Res. 33 (2009) 1101–1113.